NANO LETTERS

2007
Vol. 7, No. 5
1172−1177

Si Nanowires as Sensors: Choosing the Right Surface

Cedric R. Leão, Adalberto Fazzio, and Antônio J. R. da Silva*

Instituto de Física, Universidade de São Paulo, CP 66318, 05315-970 São Paulo, SP, Brazil

Received December 7, 2006; Revised Manuscript Received February 17, 2007

ABSTRACT

We show, using ab initio calculations based on density functional theory, that for hydrogen-passivated Si nanowires (SiNWs), the relative contribution of surface atoms to the band-edge states varies according to the way these surface atoms are bonded to the core ones. The largest influence occurs when these bonds are oriented along the wire's growth direction, which occurs either on the symmetric (001) 1×1 or the monohydrated (111) 1×1 surfaces. These results are obtained for wires grown along the [110] direction, with hexagonal cross-sections and facets corresponding to (111) and (001) planes, as observed experimentally. Their diameters range from about 10 to 35 Å. On the basis of our results, we propose that particular facets should be more appropriate to be functionalized in order to build SiNW-based sensors. As an example, we have investigated the effect of NH_2 adsorbed on some of these surfaces on the electronic structure of these wires.

Some of the most promising nanostructures for the development of new devices are semiconductor nanowires (NWs). These have been grown out of type-IV, III−V, and II−VI materials, with diameters going all the way down to 3 nm.[1,2] Many devices have already been made out of these materials, and for Si in particular, the fabrication of highly efficient field effect transistors and diodes[3,4] as well as p−n junctions[5] have been reported. These Si NWs are usually grown via a vapor−liquid−solid (VLS) technique, and Au/Si eutectic alloy droplets are the key ingredients that basically control the diameter of the Si wires. The very small diameter NWs, in the range between 3 and 10 nm, are usually grown along the [110] direction, and they present a hexagonal cross-section.[2] They usually have an oxide as a surface terminator.

One of the possible applications of these wires is on highly accurate nanoscale sensors. For such use, the surface of these systems would usually be functionalized with a receptor that, for example, would make the transport properties of the wire sensitive to the binding of a certain molecule. Thus, it might be necessary to etch the oxide off, chemically attach the receptors to the exposed Si surface, and saturate the remaining Si dangling bonds with H atoms. The usual idea is that, through the binding at the surface, some changes will be caused in the NW electronic structure such as via introduction of dopant levels or charge transfer. These techniques have already been experimentally applied to SiNWs.[6,7] In the first work, bundles of HF-etched and oxide-covered SiNWs were shown to have their electrical resistances responding in dramatically different manners upon exposure to ammonia gas. In the second work, Boron-doped amine and oxide-functionalized SiNWs were used as detectors of different biological and chemical species.[7]

In the present paper, we show, using state-of-the-art first principles calculations, that different surfaces can have quite different contributions to the density of states either at the valence-band maximum (VBM) or at the conduction-band minimum (CBM). This can also depend on the particular way the NW is terminated. This feature may be quite important for the design of sensors; it may be judiciously used in order to obtain better sensors by binding the receptors at some surfaces and not others. All of our wires are grown along the [110] direction, as were 95% of the wires, with diameters ranging from 3 to 10 nm found.[2,8] They have a hexagonal cross-section formed by the intersection of (111) and (001) planes, also as observed experimentally. Our study was divided into different categories of SiNWs: the first one consisted of wires whose (111) facets were fully saturated by three H atoms. It is worth mentioning here that such termination is unusual for infinite planar (111) Si surfaces, as it contradicts the prescriptions of Wulf's law (see, for example, the review paper ref 9), which prescribes that the cleavage planes are such as to cut as few bonds as possible: one bond, in the case of the (111) surfaces. Despite that, the SiH_3 groups have been observed at least on the flat parts of the (111) surface of Si wafers treated by HF etching 1%.[10] In ref 11, such termination was observed all over the (111) facet of HF-etched NWs by STM images. The authors speculate that the occurrence of the trihydrated phase on that facet is favored by the bending stress caused by the junctions of the different facets of the wires. This bending stress would weaken the backbonds in the atoms on the (111) facet,

* Corresponding author. E-mail: ajrsilva@if.usp.br.

10.1021/nl0628697 CCC: $37.00
Published on Web 04/12/2007

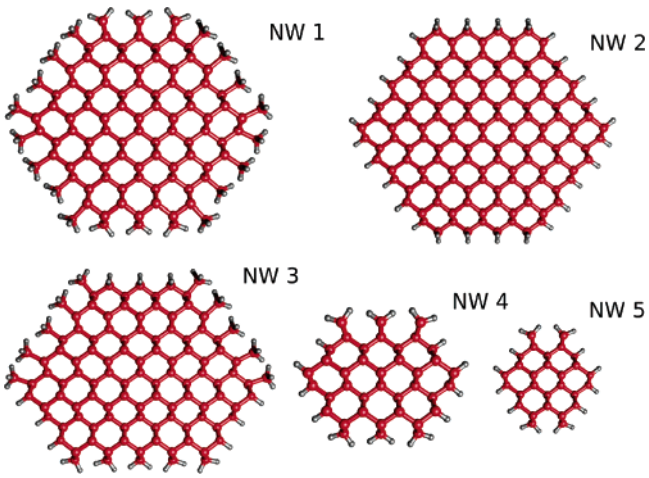

Figure 1. Cross-sections of SiNWs from the different categories studied here. All of them have their growth axis along the [110] direction. They differ in the way their facets are terminated or in their relative aspect ratios. The dark (red) spheres represent Si atoms and the light (white) ones represent H atoms.

resulting in the trihydrated structures. In ref 11, the authors also affirm that, unlike hydrogen passivated wafer surfaces, "the hydride structures on SiNWs are stable in air for several days". To our knowledge, SiNWs presenting such facets have never been theoretically studied so far. The (001) facets of these wires were passivated by two H atoms in such a way that the Si−Si bonds between the surface Si atoms and the core NW Si atoms are along the wire's growth direction, which makes the Si−H bonds perpendicular to the wire's growth direction, also according to the reports from ref 11. These are the NW1 in Figure 1. In this first category, four wires with average diameters of 12, 19, 25, and 35 Å were studied, but here we will only present the data relative to the wire of diameter $d \approx 25$ Å, whose unit cell consists of 102 Si and 60 H atoms arranged in two planes along the [110] direction. The other wires from this category present the very same trends that will be discussed here.

The second group of SiNWs display (111) facets that are obtained following the Wulf's construction. This leads to a single Si−H bond per surface Si atom instead of three Si−H bonds as before. Also, the (001) surfaces are passivated in a different scheme, where now the Si−Si bonds between the surface and core Si atoms are orthogonal to the wires' growth direction and the two Si−H bonds become aligned in rows along the wires' axes. This passivation causes a stronger electrostatic repulsion between the hydrogens on silicon atoms on neighboring planes because these H atoms are closer to each other than in the previous case (NW1). This leads to "canted bonds", as also observed on the surfaces of Si wafers. Note that, for "infinite" (mesoscopic) (001) surfaces, as there are no differences between the two directions defining the surface plane, say, X and Y, this proximity between H atoms on neighboring atomic planes is unavoidable, either along the "X" or "Y" direction. Therefore, the canted conformation is the most likely unreconstructed (001) surface in a "real" Si wafer, for example. For the surface of a SiNW, however, the same is not true. When the Si−H bonds are aligned perpendicular to the wire's growth axis, due to the "smallness" of the surface, the only tilting of Si−H bonds caused by electrostatic repulsion will happen near the surface edges. Thus there will be noncanted or symmetric (001) facets, where all the Si−H bonds are perpendicular to the wire's growth axis and this is an entirely new type of silicon surface.

The wires containing the canted (001) and the monohydrated (111) facets are the NW2 wires (Figure 1); three wires of diameters 11, 22, and 29 Å in this category were studied. Here we shall present data relative to the NW2 of $d \approx 29$ Å, whose unit cell consists of 130 Si atoms and 36 H atoms. For comparison purposes, we have also studied three "hybrid" NWs of diameters 20, 27, and 37 Å. These wires combine the above schemes of saturating the (111) and (001) facets (NW3 wires in Figure 1). This group will be represented here by the wire of $d \approx 27$ Å (109 Si and 52 H atoms in the unit cell). Finally, we have also studied two relatively small wires that do not fit exactly in any one of the previous categories, differing either in the aspect ratio between the different facets or in the way they are terminated. These wires have diameters of 14 and 12 Å (NW4 and NW5, respectively, in Figure 1). Again, as the data relative to these wires display the same trends, we chose to present only the data relative to NW4 (38 Si and 20 H atoms in the unit cell).

Given all these different ways to terminate the facets of nonreconstructed [110] SiNWs, a question that one might ask is about their energetically most favorable conformation. Such an issue has been addressed both in ref 12 and in ref 13. In the former, a method combining genetic algorithm associated with DFT calculations was employed, finding that, for all lower energy structures the (001) facets presented symmetric conformation, in agreement with the evidence from ref 11. Similarly, fully ab initio methods (DFT-LDA) were used in ref 13 for cylindrical-shaped SiNWs. These calculations pointed out the opposite result regarding the most favorable termination of the (001) facet for values of the hydrogen chemical potential above −0.23 eV. We here focus our investigation on the differences of the wires' electronic structures that these different surface conformations imply, hoping that further experimental observations might shed more light on the topic.

All of our results are based on ab initio total energy density functional theory[14] calculations. The exchange-correlation potential was treated through the generalized gradient approximation, as proposed by Perdew, Burke, and Ernzerhof.[15] The ionic core potentials were represented by nonlocal pseudopotentials,[16] whereas the spin-polarized Kohn−Sham orbitals were written in terms of a double-ζ numerical basis set plus polarization functions (DZP basis set)[17] (SIESTA code[18]). For the Brillouin zone sampling, a $(1 \times 1 \times 10)$ set was used, where the z-direction is along the wires' growth axes. All of the structures were fully optimized using the conjugate gradient algorithm until all the residual forces were smaller than 0.025 eV/Å. The supercell method with periodic boundary conditions was adopted to represent the system. The lateral sides of the supercells were (36 Å × 45 Å); this was enough to guarantee that there was no interaction between the image NWs on neighboring cells. For the largest

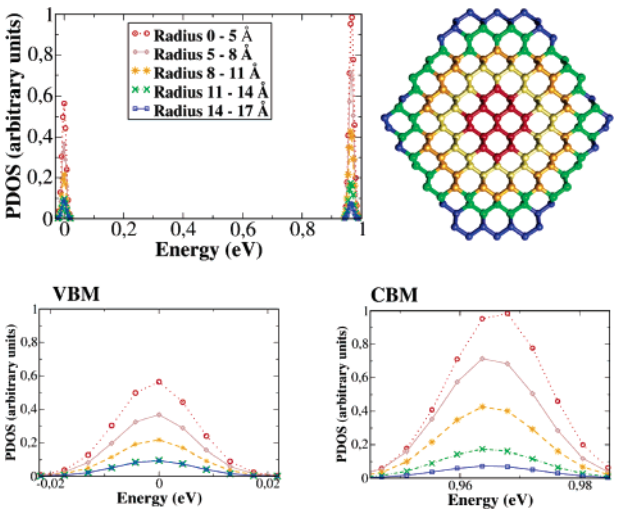

Figure 2. PDOS for the core Si atoms divided into concentric regions around the center of the wire, as shown in the structure at the right. Only the VBM and CBM states are considered. The structure is composed of the Si atoms, which are not bonded to any H atom, and they have been colored according to concentric region they belong to in order to match the PDOS curves. The curves are normalized by the total number of states (dzp orbitals) in each set and presented setting to one the peak of the PDOS associated to the innermost set of atoms at the CBM. The VBM is located at 0.0 eV. The PDOS of band-edge states have been separated and magnified at the bottom of the figure for the sake of clarity. We used a Gaussian broadening of 0.01 eV.

wires from groups NW1 and NW3, these values were enlarged to (46 Å × 54 Å). A cutoff of 200 Ry for the grid integration was utilized to represent the charge density. All of the wires had the lattice parameters along their axes optimized except the largest wires from groups NW1 and NW3. For these, we could infer from the results for the smaller nanowires that their lattice parameters are the same as the bulk's lattice parameter. We always used a single unit cell of the NW along the growth direction, which is composed of two atomic planes.

For all of the wires investigated, we have obtained a direct band gap. Besides the direct band gap, there is a secondary gap which is related to the bulk Si indirect band gap. The overall feature of the band structure is the same in every case studied here; the main changes are the difference between the direct and this indirect band gap and the particular dependence of the band gap on the diameter of the wire, which also depends on the way it is terminated.[19] These differences only come to show the importance of surface states to the formation of the band edge, as we shall demonstrate.

In Figure 2, we present the projected density of states (PDOS) for different sets of atoms for the NW1 of diameter $d \approx 35$ Å. The results for the other NWs are quite similar. In the inset of Figure 2, we present a cross-section of the wire with the atoms that are not bonded to H atoms, separated in radial rings, each one from r to $r + \Delta r$. We divide the atoms in five such rings, the first one starting at the center of the wire ($r = 0$) and ending at $r + \Delta r = 5$ Å, and all the others having $\Delta r = 3$ Å. In the graph, we show the PDOS for each one of these sets, normalized by the number of states associated with the atoms in each set. By number of states, we mean the number of dzp orbitals in each region, which in our case is 13 per Si atom. As we have also set to 1 the value of the PDOS associated with the first set of atoms at the CBM, our normalization corresponds to multiplying the PDOS in each region by the ratio between the number of atoms in the first (innermost) region and the number of atoms in the region under consideration and then dividing it by the PDOS peak associated to the innermost set of atoms at the CBM. By doing so, we ensure that the PDOS represents the relative importance of each atom in the formation of the border states instead of having regions prevailing over others because they are composed of larger amounts of atoms. As can be seen in Figure 2, both the VBM and the CBM have the largest relative contribution coming from the innermost core atoms. This could lead one to think that the Si atoms positioned at the surfaces would not have a strong influence in the gap-forming states. This, however, is not necessarily the case, as the charge isosurfaces for the gap edge states shown in Figure 3 for the (a) VBM and (b) CBM indicate. In these images, one can see that there is a charge concentration around some surface Si atoms both for the VBM and CBM states.

Moreover, we also note that, for the VBM states, there is a larger concentration of charge in the bonds between Si atoms along the wires' axes (Figure 3a, right-hand side). The highest charge isosurface on a plane intersecting these bonds is about 4 times larger than that on a plane containing only bonds between Si atoms aligned along the radial direction (Figure 3a, left hand side). For the CBM states, which have a more delocalized character, the highest charge isosurfaces in planes intersecting the wire radially (Figure 3b, left-hand side) and axially are practically equal (Figure 3b, right-hand side).

In Figure 4 we present the PDOS for NW3, and in Table 1, we give the contributions of Si atoms at different facets relative to the total core Si atoms for each of the band edges for all of the wires from NW1 to NW5. All of the curves in Figure 4 and the data in Table 1 have been normalized by the number of states (dzp orbitals) related to the atoms in each region. The heights of the PDOS curves are given relative to the VBM peak for the core atoms in each case. In other words, our normalization corresponds to multiplying the PDOS in each set by the ratio between the number of core atoms and the number of atoms in the set in question and dividing it by the peak of the PDOS of the core atoms at the VBM. The energy reference corresponds to the energy where this peak is located. The data confirm the general trends revealed by the charge density plots: the wires from group NW1 have the VBM states greatly influenced by surface atoms on the symmetric (001) facets, whereas for the wires in group NW2, the atoms on monohydrated (111) facets are the ones contributing to the formation of the VBM states. This is consistent with the above LDOS analysis (Figure 3) because the (001) facets in wires of group NW1 and the (111) facets in those of group NW2 are the ones whose Si atoms make bonds to core atoms along the wires' axes, where we observe more charge concentration in the

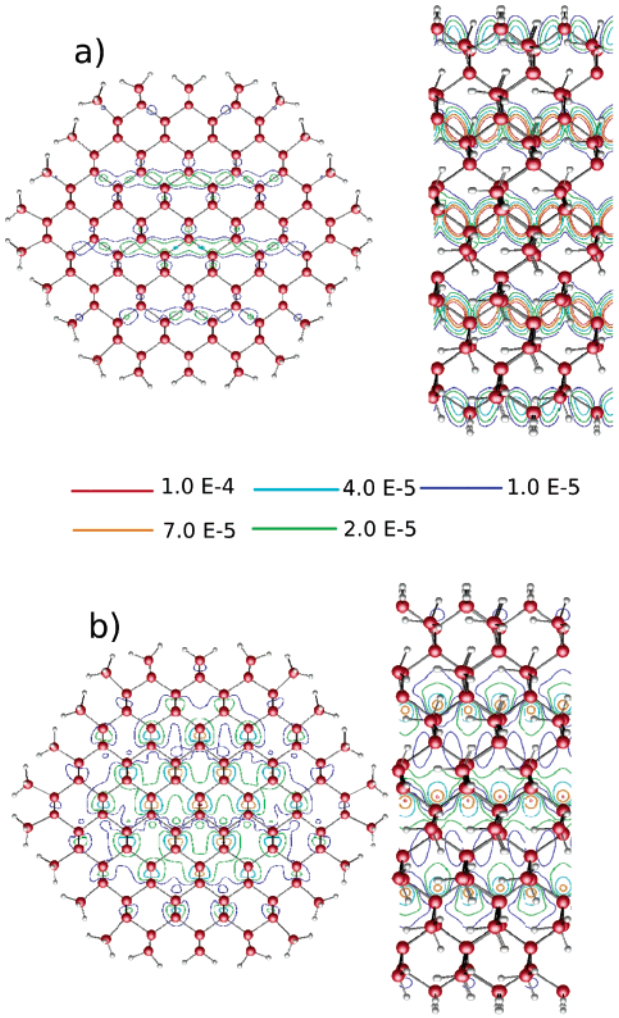

Figure 3. Charge density isosurfaces for the (A) VBM and (B) CBM states for the NW1 of Figure 1. We show charge isosurfaces on different atomic planes: planes intersecting only bonds along the wire's axis (lateral views, at the right) and also on planes containing only bonds perpendicular to the wire's growth axis (front views, at the left). The isosurfaces are in units of e/bohr.[3]

VBM states. We also note (Table 1) that the surface states seem to be more relevant in the formation of the VBM states, which present a more localized bonding character, as seen in Figure 3a, than in the CBM states, which are more delocalized (see Figure 3b). For wires from group NW1, we have noticed that, for larger diameters, the trihydrated (111) facet has a slight preponderance over the symmetric (001) at the CBM. For the wires from this group, with diameters 12 and 19 Å, this preponderance of the (111) facet over the symmetric (001) at the CBM is inverted. However, for the largest wires from group NW1, the peak of the (111) states at the CBM is less than 5% of the contribution of the core Si atoms, whereas the contribution of the symmetric (001) for the same state is almost 0.6%. For the smallest wire from group NW1, the contribution of the Si atoms on the symmetric (001) facet represents more than 37% of the contribution from core Si atoms to the CBM states, whereas the (111) states represent less than 2% of the same amount. This difference in the relative importance of surface states for the VBM and CBM, which is a general effect for all of

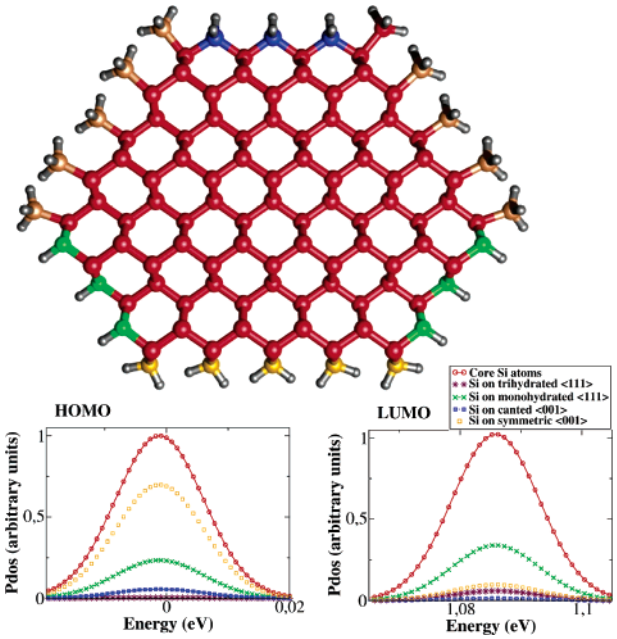

Figure 4. PDOS for the SiNW from group NW3 showing the contributions to the band edges coming from the core-atoms states and from the atoms on different facets. Only the VBM and CBM states are considered. The surface atoms have been colored in order to match the corresponding curves in the PDOS graphs. The VBM and CBM states are magnified and presented separately for the sake of clarity. The curves are normalized by the total number of states (dzp orbitals) in each set and presented here in relation to the peak of the contribution of the core Si atoms to the VBM state. The red circles refer to the PDOS associated to the core atoms; the green crosses refer to the PDOS associated to the Si atoms on the monohydrated (111) facet, whereas the brown stars refer to Si atoms on the same facet, but trihydrated. The blue squares represent the PDOS associated to the Si atoms on the canted (001) facets and the orange ones to the Si atoms on the symmetric (001) facet. The energies were shifted so that the VBM is located at 0.0 eV.

Table 1. Ratio between the Si Surface and Core Atoms PDOS for the Band-Edge States

	facets	VBM	CBM
NW1	symmetric (001)	0.757	0.235
	trihydrate (111)	0.004	0.066
NW2	canted (001)	0.046	0.034
	monohydrate (111)	0.268	0.225
NW3	canted (001)	0.054	0.017
	symmetric (001)	0.731	0.071
	monohydrate (111)	0.226	0.318
	trihydrate (111)	0.004	0.058
NW4	symmetric (001)	0.818	0.430
	monohydrate (111)	0.414	0.400
NW5	symmetric (001)	0.967	0.212
	monohydrate (111)	0.533	0.559

our wires, as displayed in Table 1, may indicate that it might be easier to affect the electronic properties of SiNWs with p-type rather than n-type dopants. Indeed, such a behavior has been experimentally observed.[20] Boron-doped SiNWs have resistivities around 1 order of magnitude smaller than SiNWs with similar doping levels of phosphorus. It is also interesting to note that it has been experimentally[21] and theoretically[22−23] verified that boron and phosphorus substi-

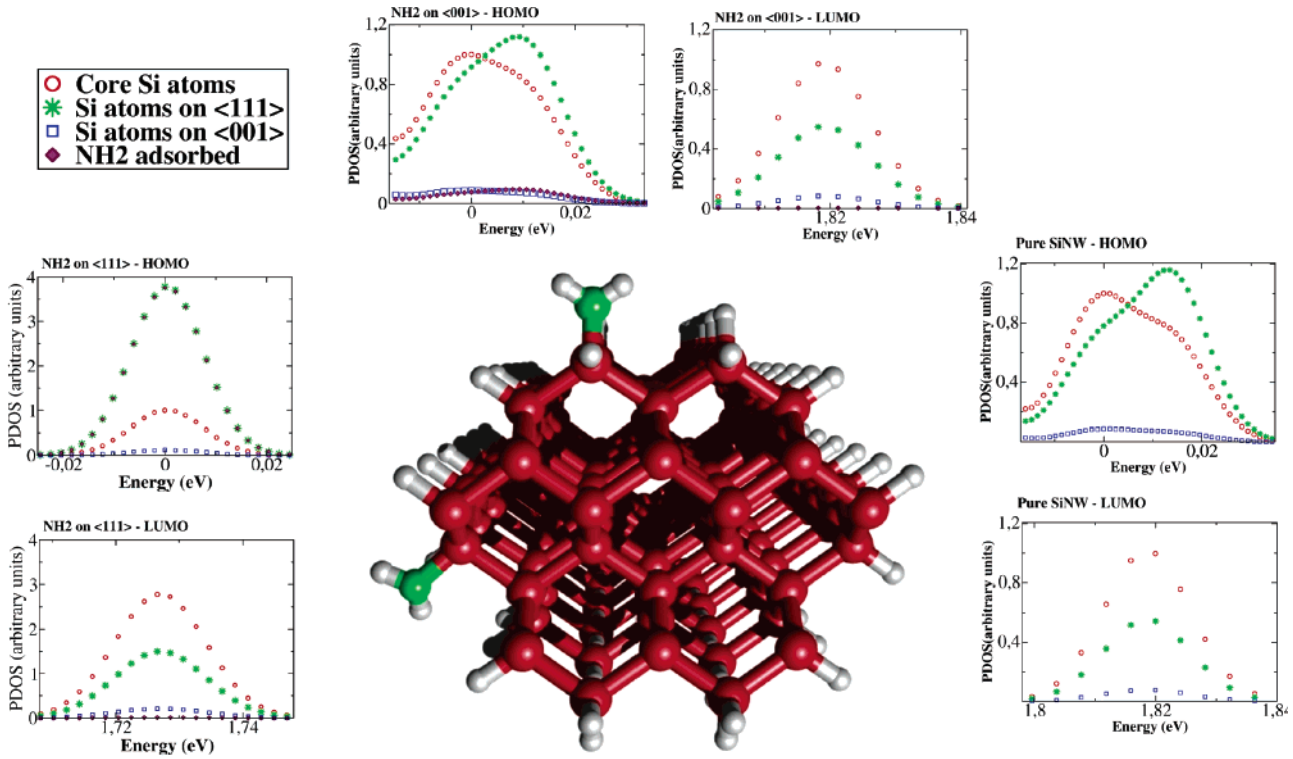

Figure 5. PDOS at a small energy window around the band-edge states of the SiNW from group NW2 in three different situations: at the right side, pure SiNW with H-passivated surfaces; on the top, the graphs refer to the same wire with one H atom from the (001) surface replaced by a radical NH_2, with all other surface dangling bonds passivated by H-atoms as in the pure wire. At the left-hand side, the NH_2 group is replacing a hydrogen atom on one of the (111) surfaces, and all other surface dangling bonds passivated by H-atoms. Red circles refer to the PDOS associated with core Si atoms; green stars are associated to the PDOS of the Si atoms on (111) surface and the blue squares to the Si atoms on the (001) facet. States originated from the NH_2 radical are indicated by brown rhombuses. The HOMO and LUMO states are magnified and presented separately for the sake of clarity. The curves are normalized by the total number of states (dzp orbitals) in each set. The energies were shifted so that the VBM is located at 0.0 eV. We used a Gaussian broadening of 0.01 eV.

tutional impurities in SiNWs will segregate at their surfaces, stressing once again the importance of studying the surface states in the formation of the band edges in these wires. Although other aspects, such as the charge mobility of carriers and different formation energies for B and P impurities in the wires, may account for that result, the relative importance of surface states in the VBM and CBM discussed above should also be taken into consideration.

The PDOS analysis for wires from groups NW1 and NW2 raise the question on whether the symmetric (001) or the monohydrated (111) would be the dominant facet if both were present in the same structure. Therefore, a similar analysis for wires from groups NW3 and NW5 was performed, see Figure 4 and Table 1. The answer is that not only they still prevail in comparison to the canted and trihydrated facets (NW3), but also they interchange the dominant role for the VBM and CBM states in wires from groups NW4 and NW5. The features displayed in the PDOS of NW4 are analogous to the ones observed in the PDOS for NW5, even though the relative aspect ratios of the facets (001) to (111) are quite different in them. This interesting effect indicates that the dominance of surfaces in relation to others is a rather robust property as well as that different facets might be the suitable ones to functionalize depending on what kind of doping one is seeking for. Therefore, we conclude that both the trihydrated (111) and the canted dihydrated (001) facets are electronically of little relevance for SiNWs. Effective mass analyses carried out in ref 13 indicate that apparently the 2×1 reconstruction of the (001) facets does not change this situation except maybe for very small ($d \approx 11$ Å) wires.

To have a more direct indication of the effects described above, we have actually connected some "foreign" groups to the different facets and analyzed the changes in the electronic structure thus achieved. Substitutional impurities in the wires,[22−23] although of being of paramount interest, would not set the matters so precisely as one could always argue that eventual modifications in the electronic structure are due to the chemical environment these impurities are embedded in, rather than consequences of, effects from the surfaces as a whole. Inspired by the experimental work of ref 6, we chose to adsorb a simple radical group, NH_2, on these facets (one at a time), removing a hydrogen atom from them (Figure 5). We have adsorbed NH_2 on both the (canted) (001) and (monohydrated) (111) facets of a wire from group NW2, whose radius is around 11 Å. We have also adsorbed the NH_2 group on the (symmetric) (001) and (monohydrated) (111) facets of NW5 (radius around 12 Å). To minimize the interaction between these radicals, we have doubled the unit cell of these wires, obtaining structures composed of four primitive planes. In this way, the distance between neighboring adsorbed radicals was above 7.8 Å in all cases.

To set a common unperturbed energy reference to measure the changes in the band structure of the wires, we placed an

Table 2. Shifts in the Positions of the HOMO and LUMO States of NWs 2 and 5 at the Γ Point in Relation to the Band Edges of the Pure Wire and the Variation of Their Spacing in Percentage of the Pure Wire's Band Gap

	HOMO (eV)	LUMO (eV)	Δ(HOMO−LUMO) (%)
NH_2 (001) NW2	0.069	0.059	−0.54
NH_2 (111) NW2	0.146	0.054	−5.04
NH_2 (001) NW5	−0.026	0.027	−3.78
NH_2 (111) NW5	−0.036	−0.010	−1.86

H_2 molecule distant about 8 Å from the surfaces of the wires.[24] We always observed a flat, zero-dispersion level related to this molecule. This allows us to perform a clear alignment of the levels calculated for different wires. In such a way, we observe that the NH_2 group, when attached to the canted (001) facet, yields a variation in the HOMO−LUMO spacing,[25] measured at the Γ point, which is about only 0.5% of that from the pure wire and almost 10 times smaller than the variation achieved when the same group is placed over the monohydrated (111) facet (Table 2). A direct comparison of the total energies (which is possible because, in both cases, the systems have exactly the same number of each kind of atom) shows that the structure with the NH_2 adsorbed on the monohydrated ⟨111⟩ facet yields a total energy 0.082 eV lower than when it is adsorbed on the ⟨001⟩ facet. As we would have expected, the structure result is more stable when the perturbation induced by the radical in the wire is more pronounced.

When the wire under consideration has both facets from kinds that we predicted would induce significant perturbations to the system, such as the symmetric (001) and the monohydrated (111) (as in NW5), we indeed observe significant changes in both cases. The NH_2 attached to the (001) facet of NW5 caused both an upshift of the HOMO and a downshift of the LUMO, resulting in an overall decrease of that spacing at the Γ point of nearly 4% in relation to the pure wire. When attached to the (111) facet of NW5, the net result was, as in all other cases, a decrease in the HOMO−LUMO energy difference (at the Γ point) in relation to the unperturbed wire. The variation in the HOMO−LUMO spacing when the NH_2 binds to the symmetric (001) facet was about two times larger than that when it was attached to the monohydrated (111) facet of the same wire. In Table 1, we observe that, although both facets present significant contribution to both band-edge states in NW5, it is again in the HOMO that this contribution is more relevant in comparison to the core states. We also note that the states associated to the symmetric (001) facet are dominant over those associated to the (111) facet at the HOMO, thus explaining the larger perturbation in the system when the radical was adsorbed on the dihydrated facet. Again, we performed an analysis of total energy, obtaining that, in this case, the structure with the NH_2 adsorbed on the symmetric ⟨001⟩ facet yields a total energy 0.051 eV lower than when it is adsorbed on the monohydrated ⟨111⟩. This result also agrees with the precept already discussed that the most stable structure results from the most interacting situation. Note that, in all cases, the final conformation of the NH_2 radical adsorbed on the wires were very similar, showing that these energy differences are not due to larger relaxation in some adsorption sites than in others.

In summary, our results show that each type of Si NW can have a distinct contribution at the VBM or at the CBM coming from atoms at distinct surfaces. This means that these surfaces can be used to alter the electronic structure around the band gap, and their effects will also be distinct. Thus, we propose that some surfaces might be more appropriate to be used to anchor, for example, receptors that will be bonding sites in sensor devices, which have already been implemented experimentally. We suggest that HF etching can be used in order to expose the more sensitive surfaces, which would then be functionalized. The important parameter controlling this behavior is the particular way the surface Si atoms are bonded to the core ones, and this may cause a given facet to change from electronically inert to the dominant one.

Acknowledgment. We acknowledge Brazilian agencies FAPESP and CNPq for financial support and CENAPAD-SP for computational time.

References

(1) Law, M.; Goldberger, J.; Yang, P. D. *Annu. Rev. Mater. Res.* **2004**, *34*, 83.
(2) Wu, Y.; Cui, Y.; Huynh, L.; Barrelet, C. J.; Bell, C. D.; Lieber, C. M. *Nano Lett.* **2004**, *4*, 433.
(3) Cui, Y.; Zhong, Z.; Wang, D.; Wang, W.; Lieber, C. M. *Nano Lett.* **2003**, *3*, 149.
(4) Duan, X.; Niu, C.; Sahi, V.; Chen, J.; Parce, J. W.; Empedocles, S.; Goldman, J. L. *Nature* **2003**, *425*, 274.
(5) Cui, Y.; Lieber, C. M. *Science* **2001**, *291*, 851.
(6) Zhou, Z.; Hu, J.; Li, C.; Ma, D.; Lee, C.; Lee, S. *Chem. Phys. Lett.* **2003**, *369*, 220.
(7) Cui, Y.; Wei, Q.; Park, H.; Lieber, C. *Science* **2001**, *293*, 1289.
(8) Schmidt, V.; Senz, S.; Gösele, U. *Nano Lett.* **2005**, *5*, 433.
(9) Herring, C. *Phys. Rev.* **1951**, *82*, 87.
(10) Morita, Y.; Miki, K.; Tokumoto, H. *Appl. Phys. Lett.* **1991**, *59*, 1347.
(11) Ma, D. D.; Lee, C. S.; Au, F. C.; Tong, S., Lee, S. T. *Science* **2003**, *299*, 1874.
(12) Chan, T.-L.; Ciobanu, C. V.; Chuang, F.-C.; Lu, N; Wang, C.-Z.; Ho, K.-M. *Nano Lett.* **2006**, *6*, 277.
(13) Vo, T.; Williamson, A.; Galli, G. *Phys. Rev. B* **2006**, *74*, 45116.
(14) Hohenberg, P.; Kohn, W. *Phys. Rev. B* **1964**, *136*, 864. Kohn, W.; Sham, L. J. *Phys. Rev. A* **1965**, *140*, 1133.
(15) Perdew, J. P.; Burke, K.; Ernzerhof, M. *Phys. Rev. Lett.* **1996**, *77*, 3865.
(16) Troullier, N.; Martins, J. L. *Phys. Rev. B* **1991**, *43*, 1993.
(17) Sankey, O. F.; Niklewski, D. J. *Phys. Rev. B* **1989**, *40*, 3979.
(18) Ordejón, P.; Artacho, E.; Soler, J. M. *Phys. Rev. B* **1996**, *53*, 10441. Sánchez-Portal, D.; Artacho, E.; Soler, J. M. *Int. J. Quantum Chem.* **1997**, *65*, 453.
(19) Leão, C. R.; Fazzio, A.; da Silva, A. J. R. in preparation.
(20) Cui, Y.; Duan, X.; Hu, J.; Lieber, C. *J. Phys. Chem. B* **2000**, *104*, 5213.
(21) Ma, D. D.; Lee, C. S.; Lee, S. T. *Appl. Phys. Lett.* **2001**, *79*, 2468.
(22) Fernández-Serra, M. V.; Adessi, C.; Blase, X. *Phys. Rev. Lett.* **2006**, *96*, 166805. Fernández-Serra, M. V.; Adessi, C.; Blase, X. *Nano Lett.* **2006**, *6*, 2674.
(23) Peelaers, H.; Partoens, B.; Peeters, F. *Nano Lett.* **2006**, *6*, 2781.
(24) Beckman, S. P.; Han, J. X.; Chelikowsky, J. R. *Phys. Rev. B* **2006**, *74*, 165314.
(25) We refer as HOMO and LUMO to the shallow level states introduced after the binding of the NH_2 to the wire, and which are positioned close to the bulk VBM and CBM (at the Γ point). As these levels are shallow, the use of a supercell leads to an impurity band with a dispersion of approximately 0.4 eV in all cases. This dispersion, however, neither is controlled by the direct interaction between the NH_2 species nor changes with the facets where the NH_2 is bonded, contrary to the HOMO and LUMO positions.

NL0628697